

Nuclear “pasta” phases by Quantum Molecular Dynamics

Katsuhiko Sato

The Univ. of Tokyo

Collaboration: G. Watanabe (Univ. Trent)

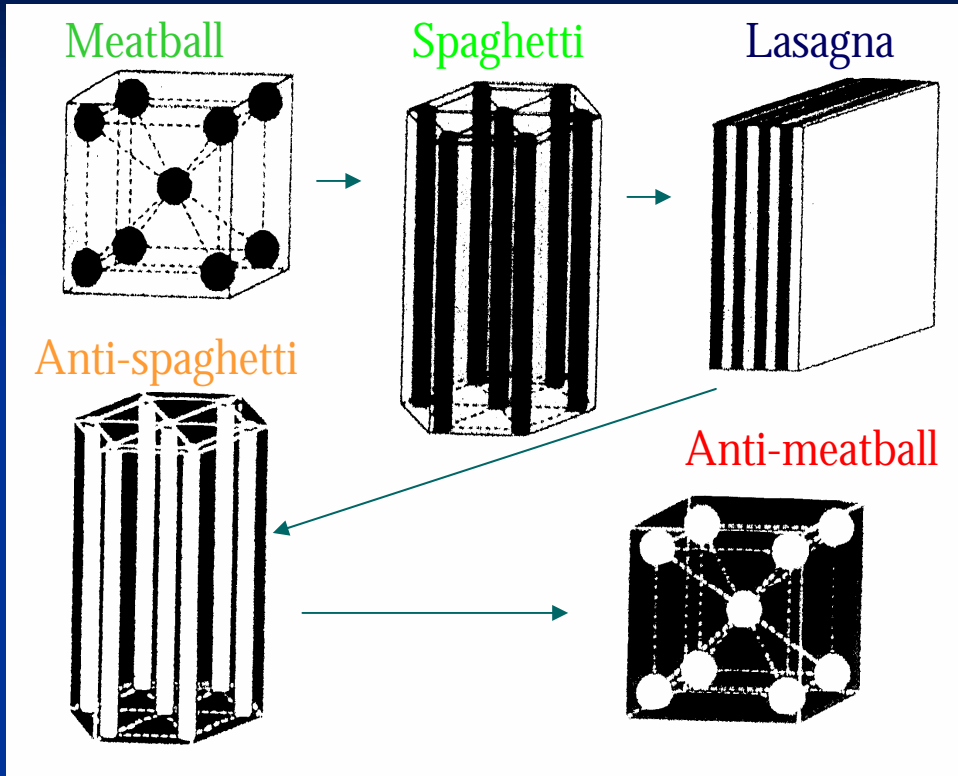
H. Sonoda (Univ. Tokyo)

K. Yasuoka (Keio Univ.),

T. Ebisuzaki (RIKEN)

T. Maruyama (JAERI)

Nuclear Pasta Structure



Oyamatsu,93

With increasing matter density, the shape of nuclei changes from sphere to cylinder, slab, cylindrical bubble and spherical bubble, successively, and eventually becomes homogeneous nuclear matter. (Ravenhall et al.,83, Hashimoto et al, 84,)

Essentially this change is described by the surface energy

$$g \equiv \frac{\text{surface area}}{(\text{volume})^{2/3}}$$

minimum principle.

Meatball
Spaghetti

Lasagna

Anti-spaghetti

Anti-meatball

"Pasta" Phases

Nuclear Pasta Structure

- Liquid drop model

Ravenhall et al., 83, Hashimoto et al., 84, Oyamatsu et al., 84,

Watanabe et al., 00, and 01, Iida et al., 01 Oyamatsu & Iida (06,)

stability and fluctuations analysis with the analogy of liquid crystal

Pethick, Potekhin, 98, Watanabe et al., 00,

- QMD (Quantum Molecular Dynamics) method

Maruyama, 98, Watanabe et al., 01, 06, Sonoda et al. 07

- Conventional MD Horowitz et al 04,, 05

complementary, large volume and large particles simulations are possible.

We improved Maruyama method and succeeded to construct the pasta structure by QMD.

QMD is very suitable method for studying **Nuclear Pasta Structure**.

- No assumptions on nuclear shapes, since nuclear system is treated in degrees of freedom of nucleons.
- Thermal fluctuations are necessarily included.

Quantum Molecular Dynamics

- Model Hamiltonian 1 (Chikazumi *et al* Phys.Rev.C 63 024602(2001))

$$\mathcal{H} = \sum_i \frac{P_i^2}{2m_i} + V_{\text{Pauli}} + V_{\text{Skyrme}} + V_{\text{sym}} + V_{\text{surface}} + V_{\text{MD}} + V_{\text{Coulomb}}$$

Kinetic Energy

Pauli Potential

Nuclear Force

Coulomb Energy

The **surface term**, which depends on the density gradient, is added to the original Maruyama model in order to make the surface of nuclei smooth. In the original model, the surface of large nuclei are slightly bumpy.

- Model Hamiltonian 2 (Maruyama *et al* Phys.Rev.C 57 655(1998))

The original model without the surface term.

Equations of Model Hamiltonian 1

$$\mathcal{H} = \sum_i \frac{P_i^2}{2m_i} + V_{\text{Pauli}} + V_{\text{Skyrme}} + V_{\text{sym}} + V_{\text{surface}} + V_{\text{MD}} + V_{\text{Coulomb}}$$

(Chikazumi *et al* Phys.Rev.C 63 024602(2001))

Definition of densities

$$\begin{aligned}\langle \rho_i \rangle &\equiv \sum_{j(\neq i)} \rho_{ij} \equiv \sum_{j(\neq i)} \int d^3\mathbf{r} \rho_i(\mathbf{r}) \rho_j(\mathbf{r}) \\ \langle \tilde{\rho}_i \rangle &\equiv \sum_{j(\neq i)} \tilde{\rho}_{ij} \equiv \sum_{j(\neq i)} \int d^3\mathbf{r} \tilde{\rho}_i(\mathbf{r}) \tilde{\rho}_j(\mathbf{r}) \\ \rho_i(\mathbf{r}) &= \frac{1}{(2\pi L)^{3/2}} \exp\left\{-\frac{1}{2L}(\mathbf{r} - \mathbf{R}_i)^2\right\} \\ \tilde{\rho}_i &= \frac{1}{(2\pi \tilde{L})^{3/2}} \exp\left\{-\frac{1}{2\tilde{L}}(\mathbf{r} - \mathbf{R}_i)^2\right\} \\ L &= 1.95\text{fm}^2, \tau = 1.33333, \tilde{L} = \frac{(1 + \tau)^{1/\tau}}{2} L\end{aligned}$$

Pauli potential

$$V_{\text{Pauli}} = \frac{C_p}{2(q_0 p_0 / \hbar c)^3} \sum_{i,j(\neq i)} \exp\left[-\frac{|\mathbf{R}_i - \mathbf{R}_j|^2}{2q_0^2} - \frac{|\mathbf{P}_i - \mathbf{P}_j|^2}{2p_0^2} \right] \delta_{\tau_i \tau_j} \delta_{\sigma_i \sigma_j}$$

$C_p = 115.0\text{MeV}, p_0 = 120.0\text{MeV}, q_0 = 2.5\text{fm}$
 τ_i : isospin, σ_i : spin

Skyrme potential

$$V_{\text{Skyrme}} = \frac{\alpha}{2\rho_0} \sum_i \langle \rho_i \rangle + \frac{\beta}{(1+\tau)\rho_0^\tau} \sum_i \langle \tilde{\rho}_i \rangle^\tau$$

$\alpha = -121.9\text{MeV}, \beta = 197.3\text{MeV}$

Symmetry potential

$$V_{\text{sym}} = \frac{C_{s0}}{2\rho_0} \sum_{i,j(\neq i)} (1 - 2|c_i - c_j|)\rho_{ij}$$

$C_{s0} = 25.0\text{MeV}, c_i : \text{isospin}$

Surface potential

$$V_{\text{surface}} = \frac{V_{\text{SF}}}{2\rho_0^{5/3}} \sum_{i,j(\neq i)} \int d^3\mathbf{r} \nabla \rho_i(\mathbf{r}) \nabla \rho_j(\mathbf{r})$$

$V_{\text{SF}} = 20.68\text{MeV}$

Momentum dependent potential

$$V_{\text{MD}} = \frac{C_{\text{ex}}^{(1)}}{2\rho_0} \sum_{i,j(\neq i)} \frac{1}{1 + \left(\frac{|\mathbf{P}_i - \mathbf{P}_j|}{\mu_1 \hbar}\right)^2} \rho_{ij} + \frac{C_{\text{ex}}^{(2)}}{2\rho_0} \sum_{i,j(\neq i)} \frac{1}{1 + \left(\frac{|\mathbf{P}_i - \mathbf{P}_j|}{\mu_2 \hbar}\right)^2} \rho_{ij}$$

$C_{\text{ex}}^{(1)} = -258.5\text{MeV}, C_{\text{ex}}^{(2)} = 375.6\text{MeV},$
 $\mu_1 = 2.35\text{MeV}, \mu_2 = 0.4\text{MeV}$

Coulomb potential

$$V_{\text{Coulomb}} = \frac{e^2}{2} \sum_{i,j(\neq i)} \left(\tau_i + \frac{1}{2}\right) \left(\tau_j + \frac{1}{2}\right) \iint d^3\mathbf{r} d^3\mathbf{r}' \frac{1}{|\mathbf{r} - \mathbf{r}'|} \rho_i(\mathbf{r}) \rho_j(\mathbf{r}')$$

● **These Hamiltonians include free parameters, 14 in Model 1 , and 13 in Model 2.**

● The values of these parameters are determined to reproduce the saturation properties of symmetric nuclear matter, and the binding energy and rms radius of stable nuclei.

Simulation settings

Eq. Motion of nucleons in QMD

$$\dot{\mathbf{R}}_i = \frac{\partial \mathcal{H}}{\partial \mathbf{P}_i} - \xi_R \frac{\partial \mathcal{H}}{\partial \mathbf{R}_i},$$

$$\dot{\mathbf{P}}_i = -\frac{\partial \mathcal{H}}{\partial \mathbf{R}_i} - \xi_P \frac{\partial \mathcal{H}}{\partial \mathbf{P}_i}.$$

Ground state is obtained by cooling of hot matter by frictional relaxation, the time scale of the cooling $\sim O(1,000\text{--}10,000)$ fm/c,

much larger than

$$\tau_{\text{relax}} \equiv \frac{\text{length scale of inhomogeneity}}{\text{sound velocity}} \\ \sim \frac{10\text{fm}}{0.1c} \sim 100\text{fm}/c$$

Simulation Settings

2,048 or 10,976 nucleons in simulation box.
Periodic boundary condition.
Proton fraction $x = n/(p+n) = 0.3$.

Computation: RSCC (RIKEN Super Combined Cluster) with

MD GRAPE (the pipeline processing module for calculating the forces between particles, originally developed for the gravitational N-body problem)

CPU time to get one model ; 2 ~ 3 weeks for spherical cases (lower density cases)

1. ~ 1.5 months for **Spaghetti and Lasagna** phases (higher cases).

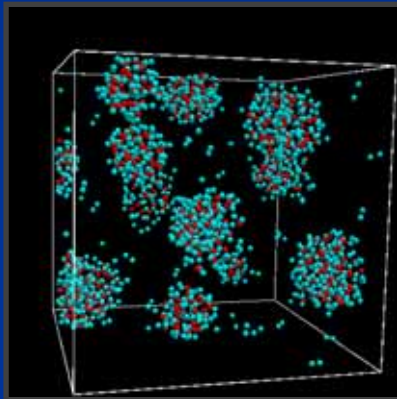
Pasta at zero temperature

Cooling of hot nuclear matter (~ 10 MeV) below 0.1 MeV

Model 1

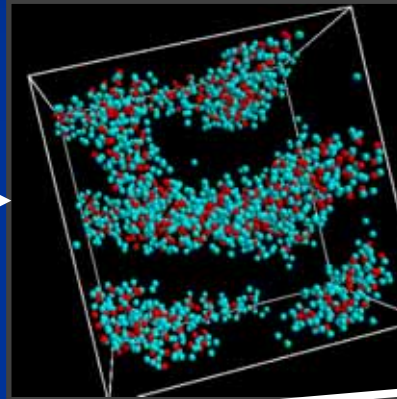
Sphere

$0.100 \rho_0$



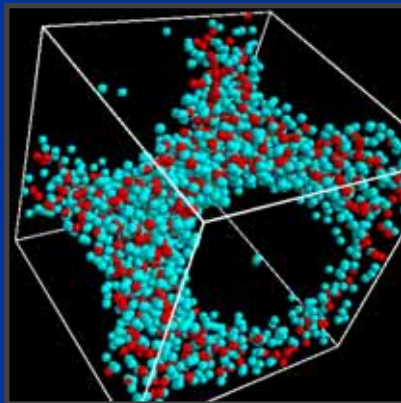
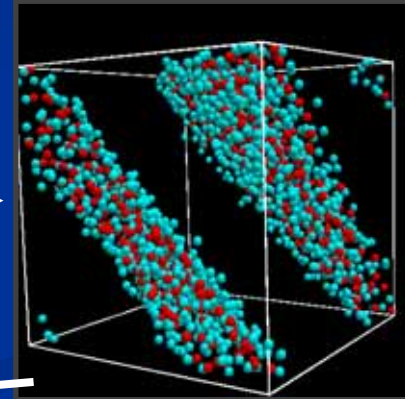
cylinder

$0.200 \rho_0$

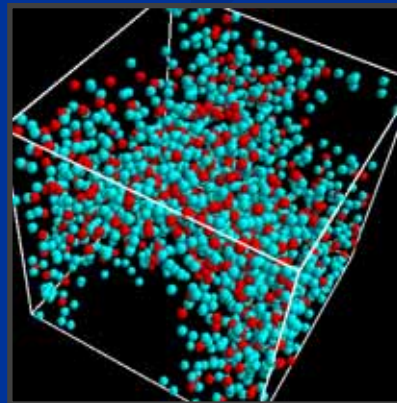


Slab

$0.393 \rho_0$



cylinder-like Holes $0.490 \rho_0$



Spherical Holes $0.575 \rho_0$

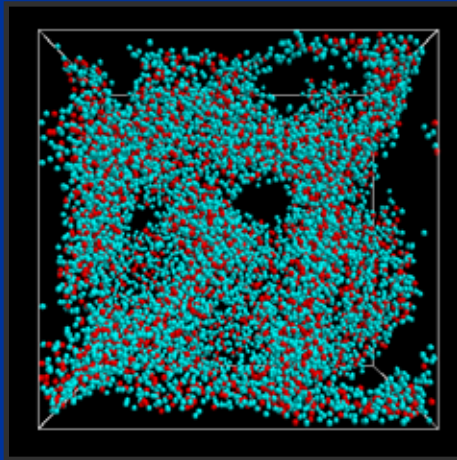
Red : Protons
Blue: Neutrons

$\rho_0 = 0.168 \text{ fm}^{-3}$
(Nuclear density)

Sponge-like Structure

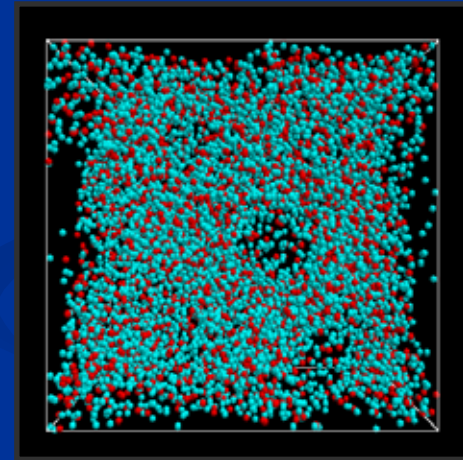
Between cylinder and slab, slab and cylinder-like holes
Multiply connected “Sponge-like” structure appears

Between cylinder and slab



10976 nucleons at 0.3 ρ_0

Between slab and cylinder holes



10976 nucleons at 0.45 ρ_0

These intermediate phases at least meta-stable

Minkowski Functionals

A powerful tool for morphological analysis

Euler characteristic

$$\chi = \frac{1}{2\pi} \int_{\partial} G dA$$

$$= (\text{number of isolated regions}) - (\text{number of tunnels}) + (\text{number of cavities})$$

About a surface of a body K in 3D space

mean curvature $H = (\kappa_1 + \kappa_2)/2$

Gaussian curvature $G = \kappa_1 \kappa_2$

κ_1, κ_2 : principal curvatures



$$\chi = 9$$



$$\chi = 3 - 3 = 0$$



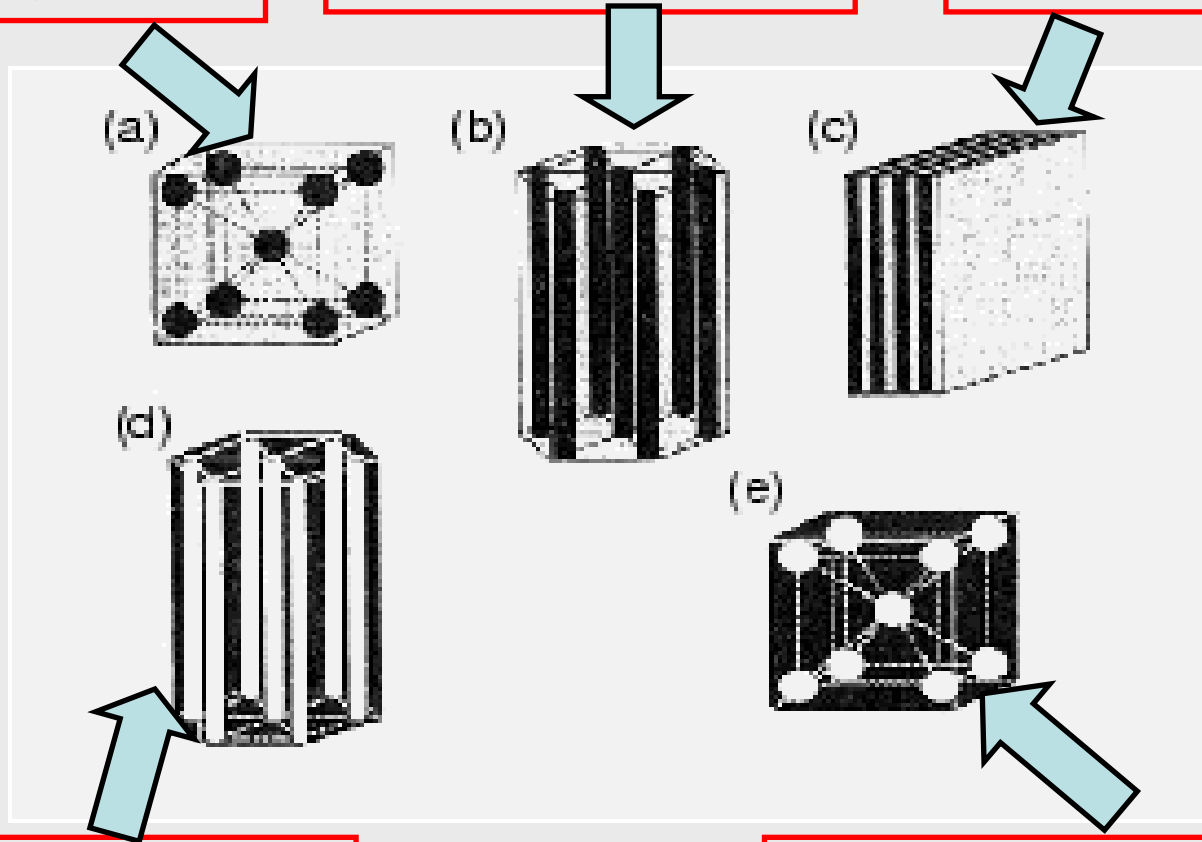
$$\chi = 1 - 5 = -4$$

Pasta phases are discriminated by H and χ .

SP:H>0, $\chi > 0$

C:H>0, $\chi = 0$

S:H=0, $\chi = 0$



CH:H<0, $\chi = 0$

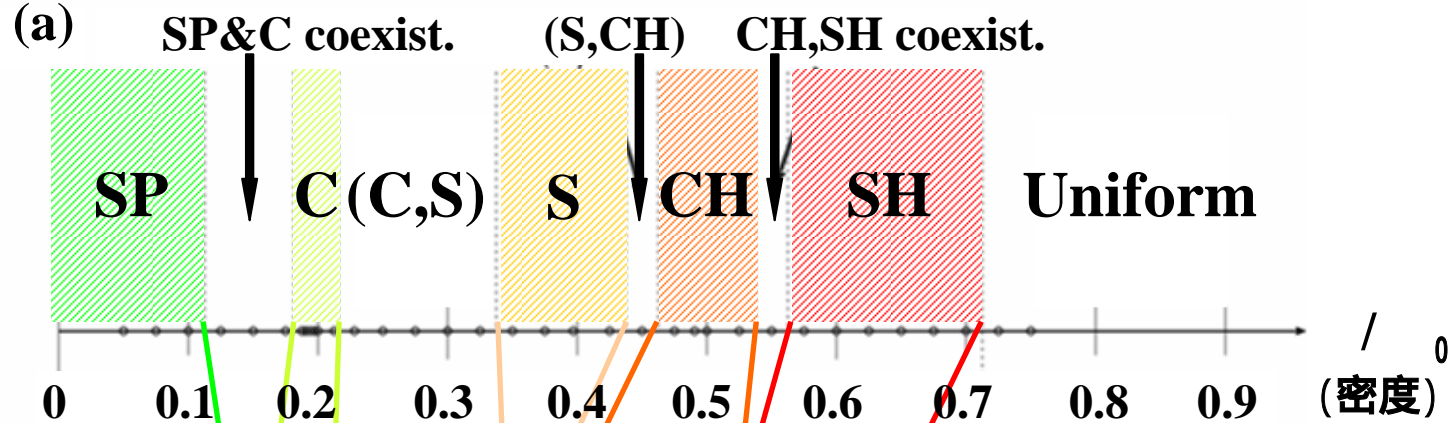
SH:H<0, $\chi > 0$

<0 ... Sponge-like Structure

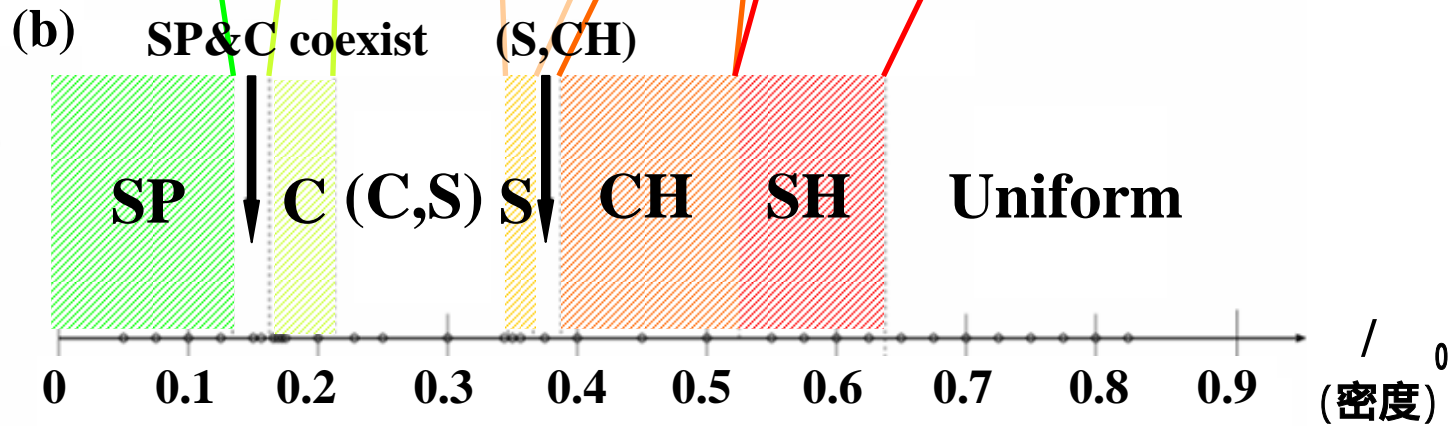
Phase diagram at zero temperature

Sphere Rod Slab Rod-like bubbles Spherical bubbles Uniform matter

Model 1



Model 2



SP: sphere S: slab SH: spherical hole
 C: cylinder CH: cylindrical hole (,): intermediate

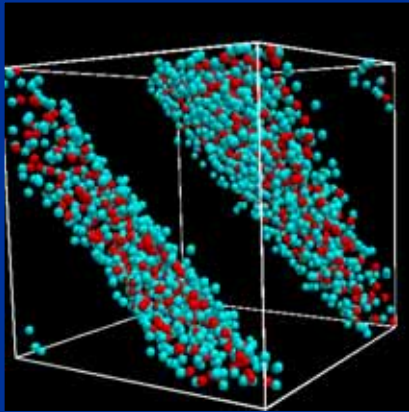
Melting density of the pasta in Model 1 is 0.7 nuclear density, higher than that of Model 2, 0.65 nuclear density by the effect of surface term.

Pasta at finite temperatures

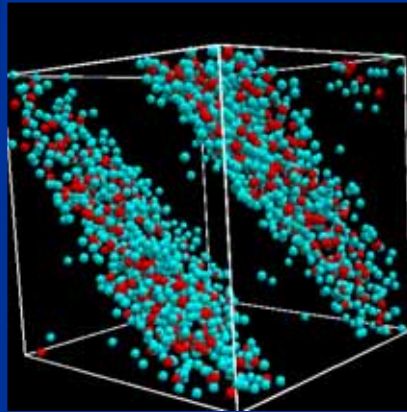
Model 1

0.393 ρ_0 (Slab nuclei at zero temperature)

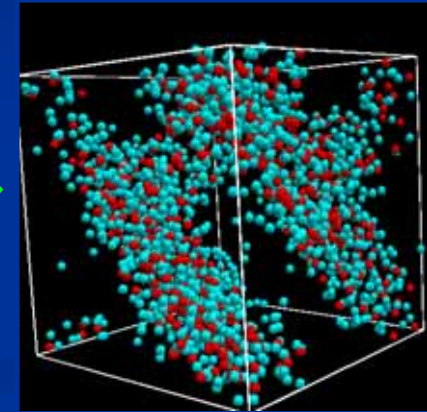
T= 0 MeV



T= 1 MeV



T= 2 MeV



Slab Nuclei

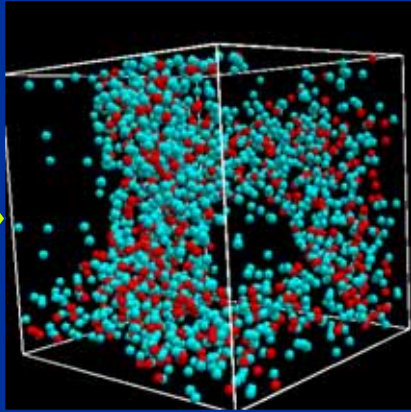
Evaporated Neutrons

Connected Slab

dripped neutrons Increases
nuclear surfaces become more diffusive

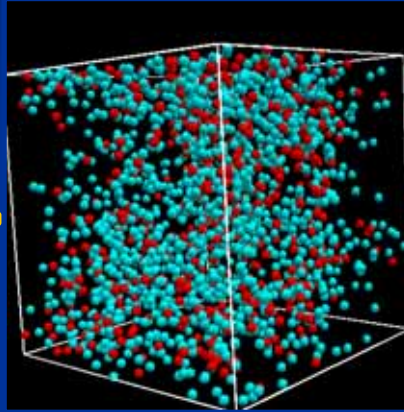
Pasta at finite temperature

T=3MeV



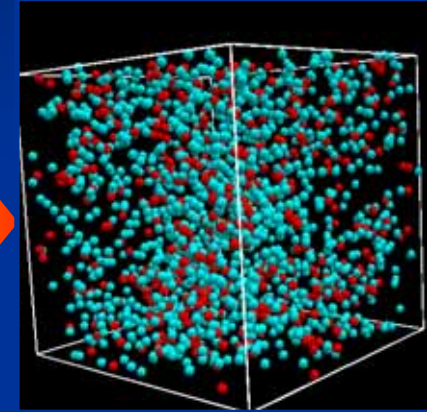
cylindrical hole-
like structure

T=5MeV



Cannot identify
nuclear surface

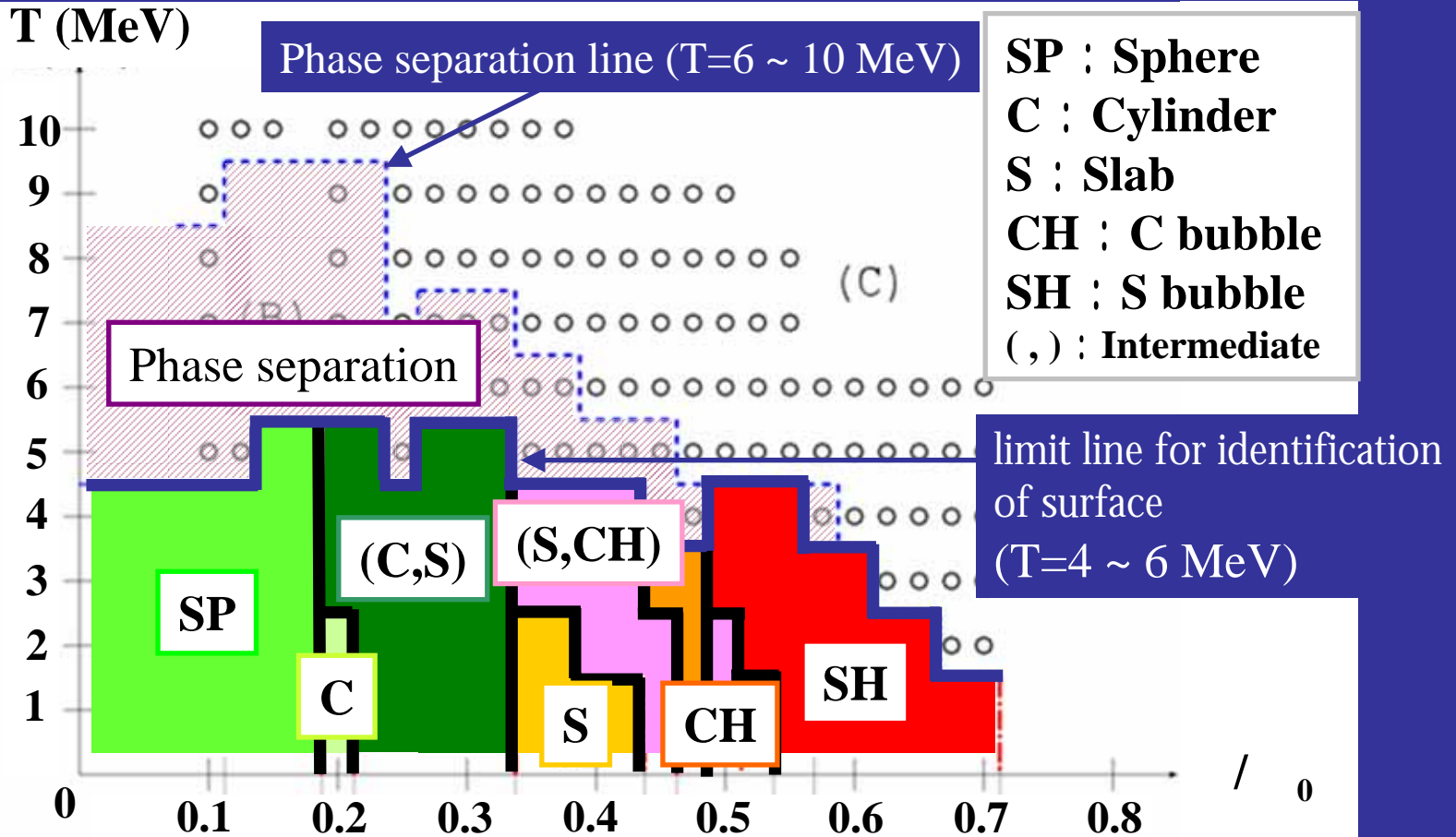
T=6MeV



Phase separation
disappears

Phase transition, Melting surface, Dripped protons,
Disappearance of phase separation occur successively

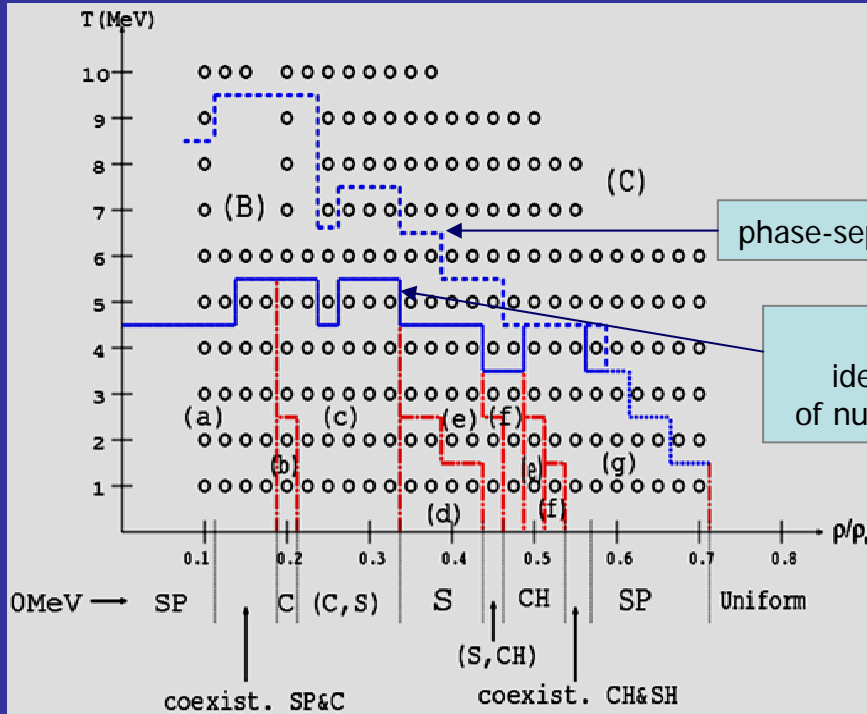
Phase diagram at finite temperatures



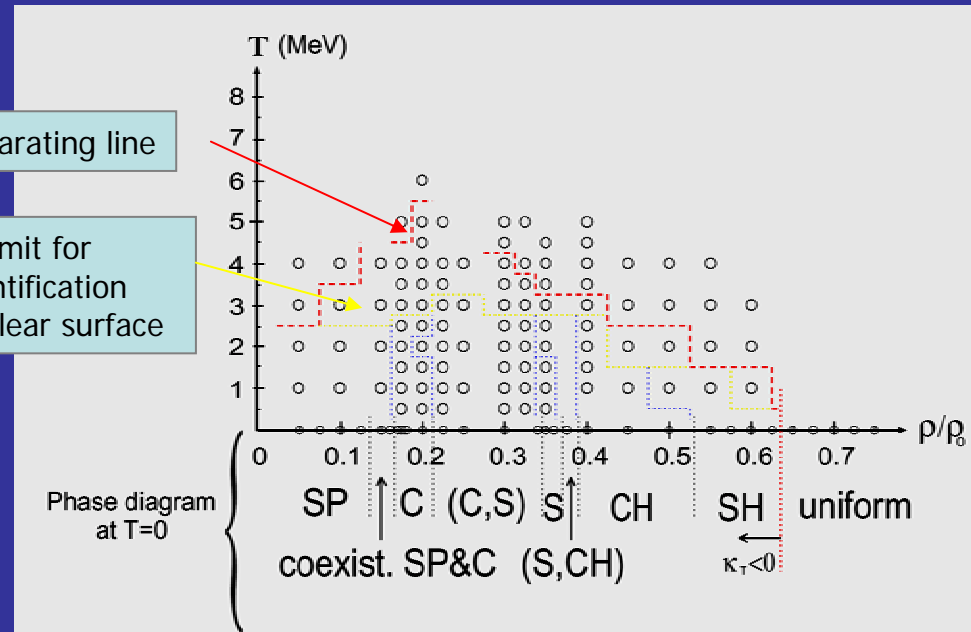
Thermal fluctuation increases volume fraction of nuclei.
 Above $T=4 \sim 6$ MeV, cannot identify surface.
 At $T=6 \sim 10$ MeV, Liquid-gas phase separation.

Comparison of Phase diagrams between two models

Model 1



Model 2



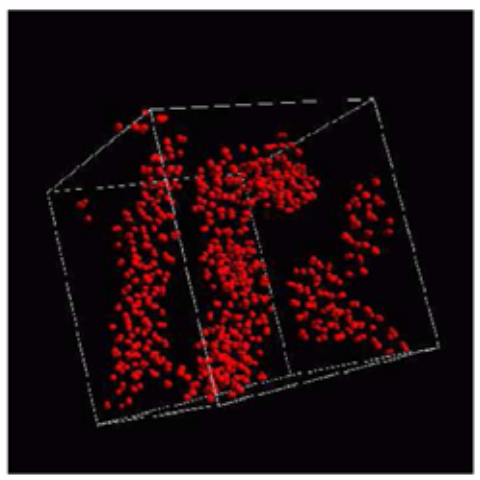
Nuclear pasta remains in higher temperature in Model 1 :

limit for identification of nuclear surface: $T=4 \sim 6$ MeV (Model 1), $2 \sim 3$ MeV (Model 2)

Phase separation line: $T=6 \sim 10$ MeV , $3 \sim 5$ MeV

Case of $X=p/(p+n)=0.1$, Model 2

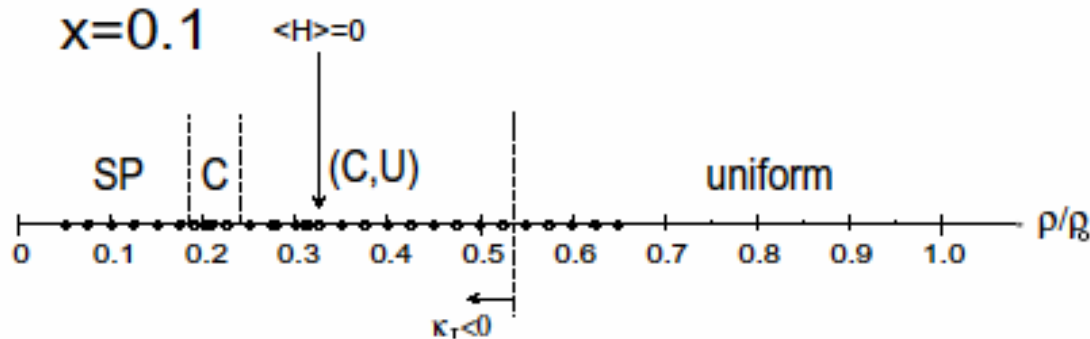
(deep side of inner crust of neutron stars)



The proton distribution of cylinder phase at $\rho = 0.2 \rho_0$ and $T=0.1\text{MeV}$.

Neutrons which spread over the whole space are not depicted in this figure.

Phase diagram



Spherical and cylindrical phase are only observed in $0.18- 0.53 \rho_0$.

No pasta phases are observed in densities higher than $0.53 \rho_0$

More systematic survey of the nuclear pasta phases of $x=0.1$ is under progress.

Neutrino Opacity of Pasta Phases

Sonoda et al PR C, 2007

Neutrino transport

--- a key element for success of supernovae

- Neutrinos are trapped in collapsing phase by coherent scattering with nuclei (K.Sato,75)
Lepton fraction , Y_{lep} , affects EOS.

How pasta phases change neutrino transport in collapsing cores ?

Pioneering investigation were done by Horowitz group (04,.....).

Neutrino cross section of neutrino-Pasta

Cross section of neutrino-nucleon system due to coherent scattering

$$\frac{1}{N} \frac{d\sigma}{d\Omega}(\mathbf{q}) = \frac{G_F^2 E_\nu^2}{4\pi^2} (1 + \cos\theta) \cdot c_\nu^{(n)2} \times \overline{S}(\mathbf{q})$$

Neutrino-neutron cross section

Amplification factor
(Static structure factor)

Because collapsing cores are poly-crystalline, the opacity would be well characterized by the angle-average of $\overline{S}(\mathbf{q})$.

Total transport cross section:

$$\sigma_t = \langle \overline{S}(E_\nu) \rangle \sigma_t^0$$

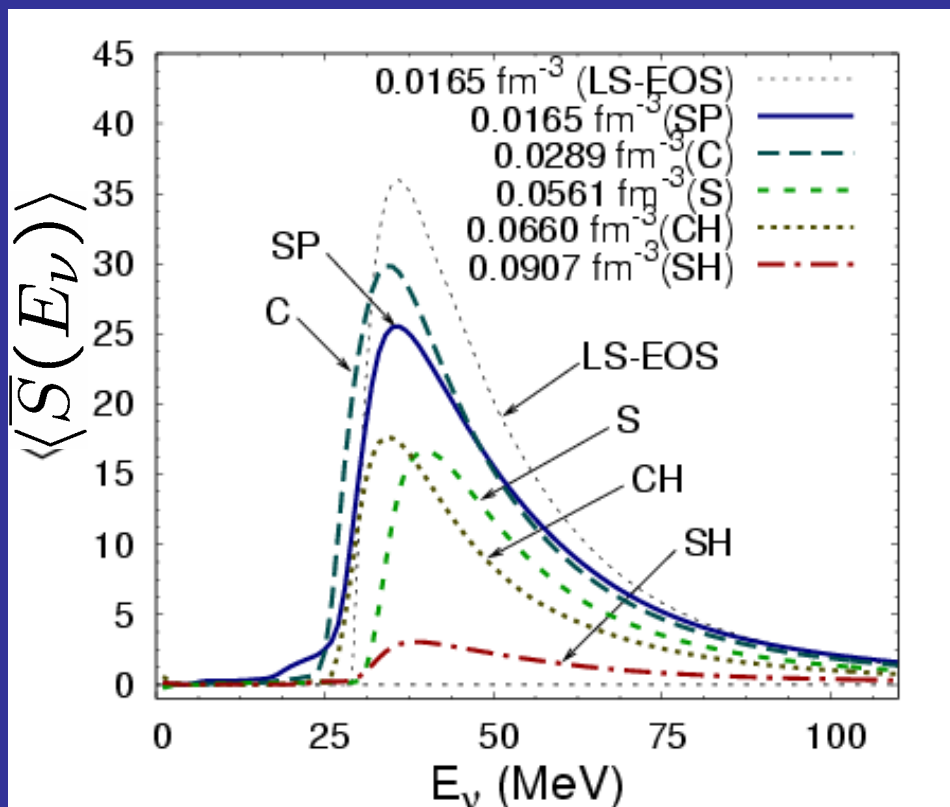
$$\sigma_t^0 = \frac{2G_F^2 E_\nu^2}{3\pi} c_\nu^{(n)2}$$

$\langle \overline{S}(E_\nu) \rangle$

Angle-averaged amplification factor by pasta structure

QMD results : change of the amplification factors with increasing density

$Y_e=0.3, T=1$ MeV



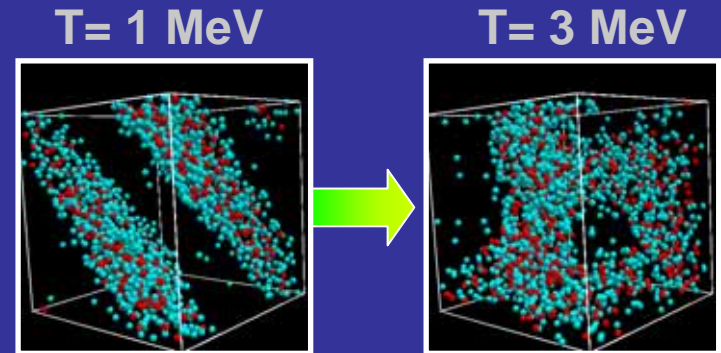
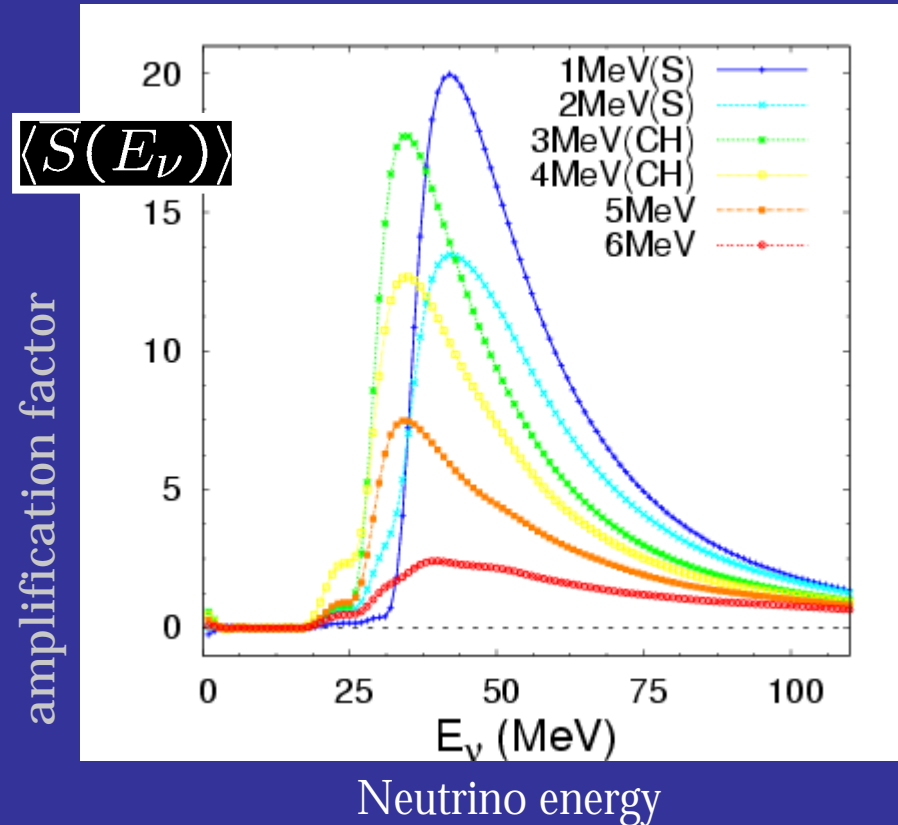
Neutrino energy

Compared with the Lattimer- Swesty model (LS-EOS),

- the energy of peaks are lower, and
 - the width of peaks are wider,
- due to lattice disorder and irregularity of nuclei.

QMD results: change of the amplification factors with increasing density

$Y_e=0.3$, $\rho=0.0660\text{fm}^{-3}$ (Slab at $T=0$)



- Peak is lowered and broader by increasing temperature due to lattice disorder and Irregularity of nuclei.
- Transition from slab(2MeV) to rod-like bubbles(3MeV) dramatically changes peak energy lower ,and peak height higher.

Difficult to discuss the effects on supernova explosion at present stage.

Summery

- Vivid pictures of nuclear pasta structure were obtained by QMD simulations.
- Difference of phase diagrams of two models available at present was investigated, but ambiguity on the dependence on nuclear potentials still remains.
- Neutrino opacity of the pasta phases described well by QMD were calculated.
- More systematic survey is under progress.